Hypergolic Performance of Dimethylthioformamide and Hydrogen Peroxide for Bipropellant Spacecraft Propulsion Systems

Ahmet Nihat Karci*† and Rose Swears*, Antony J. Musker* and Charles N. Ryan*

*University of Southampton

Boldrewood Innovation Campus, SO16 7QF, Southampton, United Kingdom

a.n.karci@soton.ac.uk · r.m.swears@soton.ac.uk · tony.musker@deltacatuk.com · c.n.ryan@soton.ac.uk

†Corresponding author

Abstract

Among the green hypergolic propellants increasingly explored as less hazardous alternatives to conventional in-space propellants like monomethylhydrazine and dinitrogen tetroxide, high-test peroxide (HTP) and novel fuels offer promising reactivity and performance. This study investigates the hypergolicity of green bipropellant combination dimethylthioformamide (DMTF)/HTP. Physical and thermochemical properties were determined, and performance metrics estimated by simulation. Drop tests evaluated ignition delay time (IDT), examining the effects of fuel additive concentration, drop height and configuration, and mixture ratio. Adding 6 wt% copper(II) chloride to DMTF significantly reduced IDT $(13.71 \pm 0.86 \, \text{ms})$. Results indicate that DMTF/HTP may be a viable green hypergolic pair.

1. Introduction

Bipropellant propulsion systems consist of two liquid components, a fuel and an oxidiser, stored separately and mixed in a combustion chamber where they ignite either spontaneously or with the help of an ignition system. They are an integral part of numerous space missions, including orbital satellites, interplanetary spacecraft and probes [1].

Hydrazine-based fuels are widely used in spacecraft chemical propulsion, with bipropellant systems commonly employing combinations of monomethylhydrazine (MMH) and dinitrogen tetroxide (NTO). Their long-standing reputation for high performance, reliability and storability has made them the preferred choice for decades. However, Monomethylhydrazine (MMH) is classified as potentially fatal, carcinogenic, and highly toxic to aquatic life. Similarly, nitrogen tetroxide (NTO) poses fatal toxicity risks and exhibits severe environmental hazards [2, 3]. The hazards associated with MMH and NTO necessitate the use of specialised protective equipment for personnel, such as self-contained atmospheric protective ensemble (SCAPE) suits. The stringent safety protocols required for handling, storage and transportation of these propellants significantly escalate operational costs [4]. This has created a focus on developing safer, green alternatives with comparable performance, especially so as satellite subsystems are required to be cheaper. Also, Hydrazine has been on the ECHA Candidate List of Substances of Very High Concern (SVHC) for over a decade [5], due to its carcinogenicity and health hazards. This means that the use of hydrazine and hydrazine-based chemicals may be restricted in the future under the REACH regulation; however, this has been the case for at least a decade, with no significant regulatory enforcement having yet occurred.

Numerous studies in the literature have focused on the development of green hypergolic bipropellants using High-Test Peroxide (HTP) as the oxidiser. Some of these studies are summarised in Table 1, with the name (where applicable), composition, and ignition delay times on conventional drop testing and in impinging-jet injectors, of various fuels that have been tested with HTP. Common factors in fuels with fast ignition delays include amine functional groups and associated high pH, inclusion of sodium borohydride as an ignition promoter, and inclusion of metal cations known to catalyse hydrogen peroxide decomposition.

The primary aim of this study is to investigate the feasibility of using DMTF and HTP as a combination of green hypergolic bipropellants for spacecraft propulsion. Neat DMTF shows promise as an hypergolic fuel, due to its low vapour pressure and toxicity, and inclusion of amide groups, analogous to the common features of other promising hypergolics. However, little attention has been paid to DMTF as a potential green hypergolic fuel to date. To assess the potential of DMTF as a potential hypergolic fuel with HTP, its physical and thermochemical properties were investigated, and theoretical performance estimations are carried out using NASA's Chemical Equilibrium with Applications

Toble 1. Ismitian Delar	. Tima data	of Hrmanali	o Croon Engle
Table 1: Ignition Delay	/ Time data	i oi mypergon	c Green rueis.

Fuel	HTP (wt%)	Drop test IDT (ms)	Injector IDT (ms)	Ref
U.S. Navy Block 0 (methanol + 22 wt% manganese acetate)	96.8	9-13	n/a	[6–8]
Triglyme + 8 wt% NaBH ₄	88.5	10.6	9	[9, 10]
HKP110 (3-dimethylamino-propylamine + 10 wt% NaBH ₄	98	2	10	[11]
1-ethyl-3-methylimidazolium cyanoborohydride + 5 wt% NaBH ₄	95	73	n/a	[12–14]
1,2-Diaminopropane (PDA) + 7 wt% NaBH ₄	95	3.13	unclear	[15, 16]
Stock 1 (tetraglyme, tetrahydrofuran, NaBH ₄)	90	12	160^{a}	[17]
Stock 2 (tetraglyme, tetrahydrofuran, toluene, NaBH ₄)	90-98	5-16	127^{a}	[17, 18]
Stock 3 (tetrahydrofuran, diethylenetriamine, NaBH ₄)	95	9	67 ^a	[19]
1-ethyl-3-methylimidazolium thiocyanate ([EMIM][SCN])	96.1	31.7	n/a	[4, 20]
[EMIM][SCN] + 5 wt% copper(I) thiocyanate (CuSCN)	96.1	13.9	n/a	[4, 20]
Dimethylthioformamide (DMTF)	95	28.8	n/a	[21, 22]

^aResearchers specified this as 'rising time'

(CEA). Finally, the ignition potential of the propellants was examined through drop tests, and further attempts were made to reduce the IDT by incorporating additives.

2. Propellant Characterisation

2.1 Green Oxidiser: High-test peroxide

HTP (also known as rocket-grade hydrogen peroxide (RGHP) in the USA [23]) is highly concentrated (85 - 98%) aqueous hydrogen peroxide, and has been used in mono- and bipropellant rocket applications due to its relatively low vapour pressure and non-toxic exhaust and decomposition products [12]; HTP catalytically decomposes into a high-temperature mixture of steam and oxygen [24]. Unlike NTO, HTP does not produce hazardous fumes or pose severe long-term health risks from inhalation or skin exposure [25]. However, HTP, as a strong oxidiser can cause chemical burns upon contact [26].

Some physical and thermochemical properties of HTP and NTO are presented in Table 2. Key advantages of HTP over NTO as an oxidiser include its comparable density, allowing space-efficient oxidiser storage; its significantly lower vapour pressure and boiling point, improving handling safety; and its high active oxygen content (47.1%), meaning a significant portion of the propellant directly contributes to combustion. However, potential drawbacks include its higher viscosity, affecting flow behaviour; higher surface tension, slightly affecting atomisation efficiency; and high freezing point, requiring more rigorous thermal management. A well-publicised drawback of HTP is its slow decomposition on storage. This can be managed by use of stabilisers such as colloidal stannate and sodium pyrophosphate [27], or judicious selection of hardware materials. Compatible materials include low-copper aluminium alloys (especially 1060, 1160, 1260, and 5254), 300-series stainless steels, tantalum, zirconium, and various fluoropolymers, including PTFE, PFA, and PVDF, and polyethylene and Mylar [28].

Table 2: Physical and thermochemical properties of 100 wt% H₂O₂ and N₂O₄ (NTO) [29–31].

Property	$\mathbf{H}_2\mathbf{O}_2$	NTO (N_2O_4)
Active oxygen content (%)	47.1	N/A
Molecular weight (g/mol)	34.015	92.02
Density at 20 °C (g/mL)	1.450	1.448
Freezing point (°C)	-0.4	-11.2
Boiling point at 1013 mbar (°C)	150	21.2
Vapour pressure (mmHg)	6	1151
Specific heat at 25 °C (J/g·K)	2.6	1.55
Refractive index, n _{25D}	1.4067	1.434
Viscosity at 20 °C (mPa·s)	1.25	0.47
Surface tension at 20 °C (mN/m)	80.4	27.5

2.2 Physical and thermochemical properties of fuels

The comparative physical and thermochemical properties of DMTF and MMH are summarised in Table 3. MMH offers superior energetic performance, with a higher enthalpy of formation and a lower freezing point. However, DMTF exhibits a significantly higher flash point and lower vapour pressure than MMH, enhancing handling and storage safety. Its higher density and lower viscosity contribute to improved volumetric efficiency and flow behaviour, supporting its candidacy as a safer, more environmentally benign alternative.

Property	DMTF	MMH
CAS Number	758-16-7	60-34-4
Molecular Formula	C_3H_7NS	CH_6N_2
Molecular Weight (g/mol)	89.16	46.07
Freezing/Melting Point (°C)	-8.5	-52.4
Boiling Point (°C)	58 - 60	88 - 90
Vapour Pressure (mbar)	0.13	67
Density (g/cm ³)	1.047	0.875
Dynamic Viscosity (mPa·s)	0.1	0.775
Autoignition Temperature (°C)	_	182
Flash Point (°C)	99	-8
Enthalpy of Formation $\Delta H_{\text{final}}^0$ (kJ/mol)	-16	54.14

Table 3: Physical and thermochemical properties of DMTF and MMH [2, 32–36].

3. Methodology

3.1 Theoretical performance estimation by NASA CEA

This subsection presents estimated performance values for HTP and DMTF calculated using NASA CEA software. CEA theoretical background and operational guidance are documented in NASA reference publications RP-1131 and RP-1131-P2 [37,38]. In these simulations, 98 wt% HTP was used as the oxidiser, with the remaining 2 wt% assumed to be water. The frozen at throat setting was selected, as that tends to yield more realistic results for smaller rockets. Additional input parameters, such as chamber pressure (9 bar) and expansion ratio (150), were adopted from the specifications of a 10 N commercial bipropellant thruster produced by the Ariane Group [39].

3.1.1 Specific impulse and density specific impulse investigation

Figure 1 compares the vacuum specific impulse ($I_{\rm sp,vac}$) and density-specific impulse ($\rho I_{\rm sp,vac}$) of MMH/NTO and DMTF/HTP (98 wt% H_2O_2) propellant systems, as a function of oxidiser-to-fuel ratio (O/F). The $I_{\rm sp,vac}$ (solid lines; left-hand y-axis) reaches a peak of approximately 336 s for MMH/NTO near O/F = 1.8, and 316 s at O/F = 4.0 for DMTF/HTP. Despite its lower $I_{\rm sp,vac}$, DMTF/HTP demonstrates a superior density-specific impulse due to the higher density of both the fuel and oxidiser. The $\rho I_{\rm sp,vac}$ (dashed lines; right-hand y-axis) reaches a peak of approximately 394 g·s/cm³ for MMH/NTO, and 422 g·s/cm³ for DMTF/HTP. Overall, while MMH/NTO delivers higher specific impulse values, DMTF/HTP offers enhanced volumetric efficiency.

3.1.2 Effect of additives on performance indicators

Additives are often included to enable or enhance hypergolic ignition of candidate green fuels with HTP. Catalytic additives, such as copper or manganese salts, accelerate HTP decomposition, releasing heat and oxygen that support ignition. Energetic additives, like NaBH₄, react exothermically with HTP, generating sufficient heat to achieve ignition. These additives play a critical role in reducing IDT and ensuring reliable ignition performance.

As explained in subsection 4.2, CuCl₂ has been used to prepare fuel mixture with DMTF to obtain shorter IDT than pure DMTF/HTP has been provided. This subsection explains the effects of additive CuCl₂ usage on theoretical performance estimation using NASA CEA2. Therefore, the fuel mixture is simulated for three CuCl₂ wt% amounts of 3, 6 and 9. The results for vacuum specific impulse are shown in Figure 2 and for density vacuum specific impulse are shown in Figure 3.

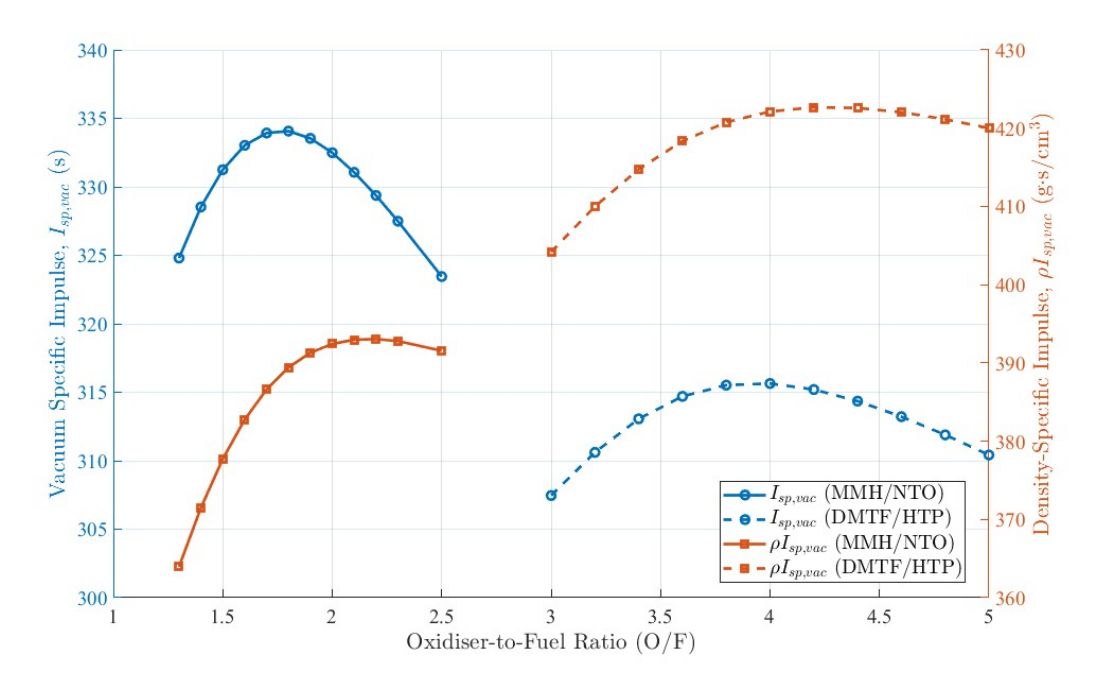


Figure 1: Theoretical Performance of DMTF & HTP (98 wt% H₂O₂ and 2 wt% H₂O) and MMH & NTO.

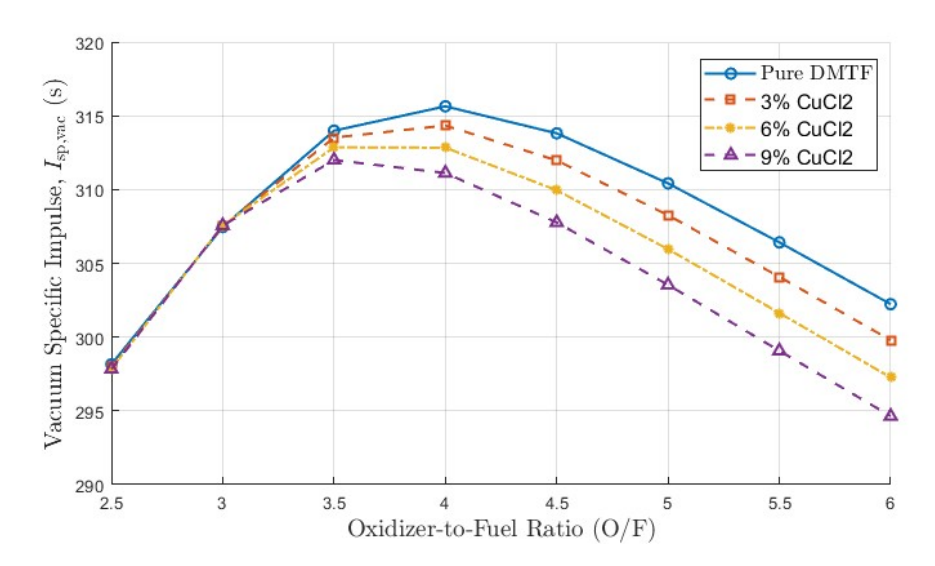


Figure 2: Effect of CuCl₂ additive in DMTF with HTP (98 wt% H₂O₂ and 2 wt% H₂O) on Specific Impulse.

For O/F below 3.5, the addition of $CuCl_2$ has no significant effect on $(I_{sp,vac})$. However, for O/F ratios above 3.5, increasing $CuCl_2$ reduces specific impulse. The peak $I_{sp,vac}$ for pure DMTF is approximately 316 s at an O/F of 4.0, whereas for 3%, 6% and 9% $CuCl_2$, the peak values decrease to 314 s, 312 s and 311 s, respectively. I_{sp} increases with increasing combustion chamber temperature and decreasing average molecular weight of exhaust products. For O/F ratios below 3.5, DMTF with $CuCl_2$ additive exhibits higher chamber temperature values than pure DMTF, compensating for the slight increase in molecular weight of exhaust products. However, for O/F ratios above 3.5, the combustion temperature of the additive-containing fuel becomes lower than that of pure DMTF. Since both parameters now act against performance, the specific impulse of the additive-containing mixture drops below that of the pure DMTF.

On the other hand, the presence of $CuCl_2$ in the fuel mixture increases the vacuum density-specific impulse ($\rho I_{\rm sp,\,vac}$). This is expected, as $CuCl_2$ has a higher density than DMTF, leading to an overall increase in the mixture's density-specific performance. The peak $\rho I_{\rm sp,vac}$ for pure DMTF is around 422 g·s/cm³, whereas with 3%, 6% and 9% $CuCl_2$, the peak values increase to 426 g·s/cm³, 432 g·s/cm³ and 434 g·s/cm³, respectively.

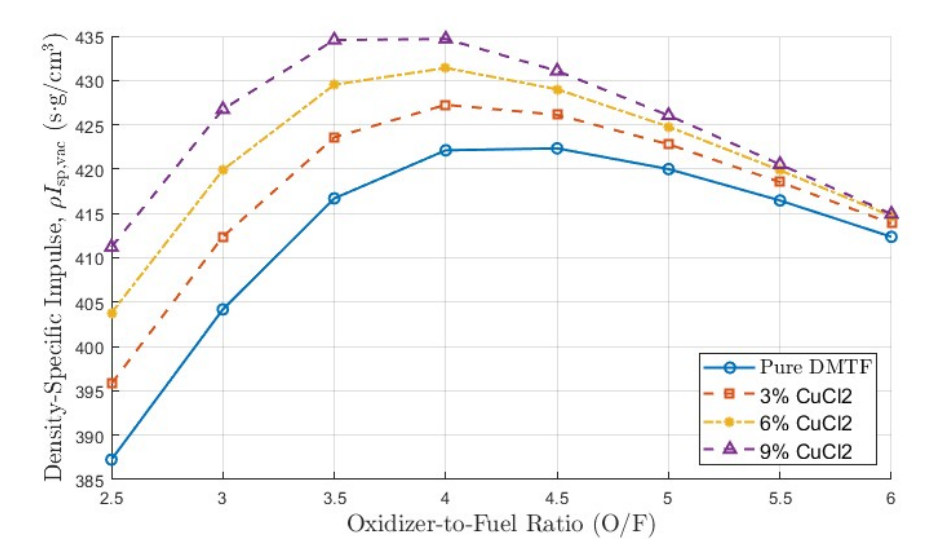


Figure 3: CuCl₂ effect on Density Specific Impulse of DMTF.

3.1.3 Exhaust products estimation by NASA CEA

Exhaust gas products at maximum I_{sp} condition were estimated using NASA CEA, after [40]. This theoretical evaluation is based on equilibrium conditions. In reality, assuming frozen flow at the throat is crucial for performance calculations, whereas a sliding equilibrium condition offers insight into theoretical chemical equilibrium behaviour. So, simulation conditions are kept the same except for equilibrium conditions. This analysis does not assume frozen flow at the throat. In both cases the exit temperature is approximately 944 K.

The exhaust products of DTMF/HTP mixture simulation are given in Table 4, and those where DMTF has 5 wt% CuCl₂ added are given in Table 5. Molecules are listed in order of mass fraction, and molecular weights are included.

Molecule	Mass Fraction	Molecular Weight (g/mol)
H ₂ O	0.56636	18.02
CO_2	0.27346	44.01
SO_2	0.12726	64.07
N_2	0.02909	28.01
H_2S	0.00183	34.08
S_2	0.00114	32.07
CO	0.00048	28.01
H_2	0.00032	2.02
S_2O	0.00003	80.13
COS	0.00002	60.07
SO	0.00001	48.06

Table 4: Mass Fractions of the Exhaust Products for DMTF/HTP.

The primary exhaust species in both cases are water vapour $(H_2O, 56\%)$, carbon dioxide $(CO_2, 27\%)$ and sulfur dioxide $(SO_2, 13\%)$, comprising 96% of products. Nitrogen (N_2) and hydrogen sulphide (H_2S) are present in smaller amounts. When 5 wt% $CuCl_2$ is added to the fuel, copper(I) sulphide (Cu_2S) and hydrogen chloride (HCl) emerge as additional exhaust species. No solid exhaust products were identified in the DMTF/HTP case. However, in the simulation with 95 wt% DMTF and 5 wt% $CuCl_2/HTP$, Cu_2S is expected to form as a solid, constituting approximately 0.6 wt% of the total exhaust products as shown in Table 5. This highlights the chemical differences between the two cases, particularly the role of $CuCl_2$ in modifying the exhaust composition. Understanding these variations is crucial for assessing their potential impact on plume characteristics and combustion performance.

Hydrogen sulfide (H₂S), carbon monoxide (CO), SO₂, HCl and Cu₂S are among the primary health concerning combustion byproducts. These compounds, listed in Table 5, are formed during injector and thruster tests and would require proper safety measures to mitigate exposure during testing on the ground.

Molecule	Mass Fraction	Molecular Weight (g/mol)
H ₂ O	0.56135	18.02
CO_2	0.27007	44.01
SO_2	0.12793	64.07
N_2	0.0287	28.01
Cu_2S	0.00569	159.16
HCl	0.00521	36.46
H_2S	0.00039	34.08
CO	0.0003	28.01
H_2	0.00019	2.02
S_2	0.00015	64.13
S_2O	0.00001	80.13

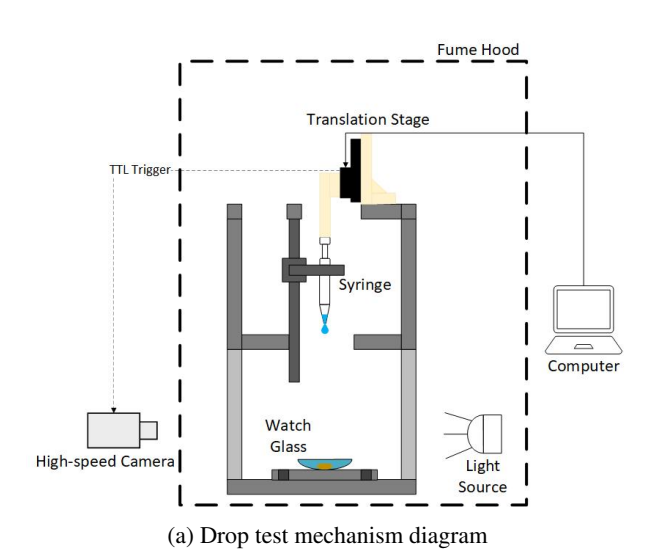
Table 5: Mass Fractions of the Exhaust Products for 95 wt% DMTF & 5 wt% CuCl₂/HTP.

3.2 Drop Test Mechanism

Drop tests are a practical and efficient method for evaluating the hypergolic potential of a fuel and oxidiser [4,41]. In these tests, a small droplet of fuel is released onto a pool or droplet of oxidiser and the reaction is observed to determine whether spontaneous ignition occurs upon contact. Although drop tests do not replicate the high-pressure and dynamic flow conditions of a thruster, they serve as a reliable first-step screening tool. Fuels that exhibit consistent and fast ignition in drop tests are considered strong candidates for further evaluation under realistic propulsion conditions.

Drop tests were performed in the Engineering Materials Lab in Eustice building at University of Southampton. The semi-automated drop test mechanism was designed and manufactured based on the design principles outlined in [11]. It is referred to as semi-automated because, while the trigger mechanism allows the drop tests to be conducted automatically, the placement of propellants and the post-test cleaning are performed manually. A diagram and actual test site image are shown in Figure 4. The drop tests were conducted under a fume hood under ambient conditions, because the primary objective was to identify new hypergolic propellant combinations.

The drop test setup was designed to ensure precise synchronisation between propellant release and high-speed camera recording. A computer-driven motorised translation stage (MTS50/M-Z8, Thor Labs, 50 mm travel range) controlled the syringe, releasing a drop of propellant while simultaneously triggering the high-speed camera using a Transistor - Transistor Logic (TTL) pulse. The TTL signal (5V, 8 mA) was generated by the Thorlab's K-Cube brushed DC servo motor controller and transmitted via a BNC coaxial cable to the trigger input of the Photron Fastcam SA3, ensuring accurate timing between droplet release and video capture. The high-speed camera settings for the experiments included a frame rate of 3000 fps and an aperture setting of f/16. Images were captured at a resolution of 768 x 768 pixels, and processed using Photron FASTCAM Viewer (PFV4). A polarisation filter was used to minimise glare.





(b) Drop test experimental setup

Figure 4: Drop test system: Diagram (left) and actual test site (right).

4. Results and Discussion

4.1 Drop Test Results

This section presents the results of the drop tests. To ensure accuracy in repeated tests conducted under identical conditions, the uncertainties in time to vapour generation (TVG) and ignition delay time (IDT) measurements have been evaluated based on the standard deviation of repeated measurements, following the method described in [42]. The device uncertainty is determined by the time resolution of the high-speed camera, which corresponds to the theoretical duration of a single frame. The total standard uncertainty is then calculated as the root sum square of the statistical and device uncertainties [42].

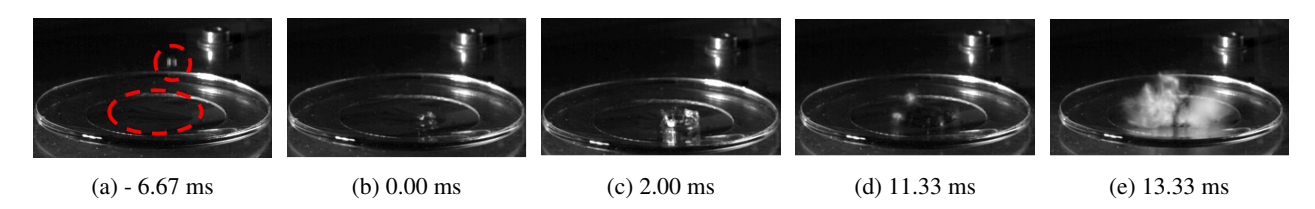


Figure 5: Snapshots of a drop test using 95.41 ± 0.27 wt% H₂O₂ and DMTF with 5 wt% CuCl₂.

Figure 5 illustrates the procedure for determining TVG and IDT in drop tests. In Figure 5(a) shows the approach of an oxidiser droplet towards the fuel on the watch glass. The fuel and oxidiser droplets are indicated with red dashed lines. Figure 5(b) captures the frame where the fuel and oxidiser first come into contact; this frame is designated as the zeroth millisecond and serves as the reference point in the calculation of both TVG and IDT. The mixture process of propellants is given in Figure 5(c). The first visible vapour formation is depicted in Figure 5(d). The IDT is similarly determined, as illustrated in Figure 5(e).

4.2 Additive concentration in the fuel mixture

Literature suggests that an IDT of approximately 15 ms is generally required to ensure safe operation during thruster tests [4, 43]. However, the IDT for the pure DMTF and HTP combination is around 27 ms. To mitigate this, $CuCl_2$ was added to the fuel mixture to shorten the delay. The corresponding results are collectively presented in Figure 6. The $CuCl_2$ concentration in the DMTF - based fuel was varied from 1 wt% to 9 wt% and each mixture was evaluated with HTP using the drop test setup. (MAT and NaBH₄ were considered as additives, but were insoluble in DMTF.) The oxidiser concentration employed in the tests was 95.41 \pm 0.27%.

Figure 6 illustrates the relationship between the $CuCl_2$ proportion in the fuel mixture (wt%) on the x-axis and time (ms) on the y-axis. Two datasets are presented: TVG and IDT, represented by blue circles and orange squares with error bars indicating statistical uncertainty over six tests.

As the $CuCl_2$ proportion increased up to 6 wt%, both TVG and IDT values decreased, down to minima of TVG = 12.13 ± 0.83 ms and the IDT = 13.71 ± 0.86 ms. However, for $CuCl_2 > 6\%$, TVG and IDT increased slightly, which can be attributed to the increased physical delay of the mixture, influenced by its viscosity and surface tension.

Higher $CuCl_2$ concentrations led to more vapour production and a brighter flame. However, at 9 wt% $CuCl_2$, the additive did not fully dissolve in DMTF, indicating that the solubility limit was reached. Figure 6 also shows that the presence of any $CuCl_2$ in the fuel mixture significantly reduces the delay between TVG and IDT. For example, at 1 wt% $CuCl_2$, TVG decreased from 18.67 ms to 15.28 ms, while IDT was reduced from 26.94 ms to 18.50 ms.

4.3 Effect of drop height

It was investigated whether drop height (the distance between the tip of the syringe and the top edge of the watch glass) had an effect on the TVG and IDT. Drop height values tested were 250 mm, 225 mm and 200 mm, constrained by the physical limitations of the drop testing apparatus.

These are shown in Figure 7, where the x-axis represents the drop height (mm), while the y-axis shows TVG (blue circles) and IDT (orange squares) in milliseconds, with error bars representing measurement variability. The impact velocities corresponding to the tested drop heights were calculated assuming free-fall motion under gravity, ignoring air resistance. For a drop height of 250 mm, the impact velocity was estimated as 2.21 m/s. At 225 mm, the velocity decreased to 2.10 m/s and at 200 mm, it further reduced to 1.98 m/s. It is apparent that average TVG and IDT values increase with decreasing drop height: at 200 mm, TVG and IDT are approximately 14.2 ms and 16.0 ms, respectively.

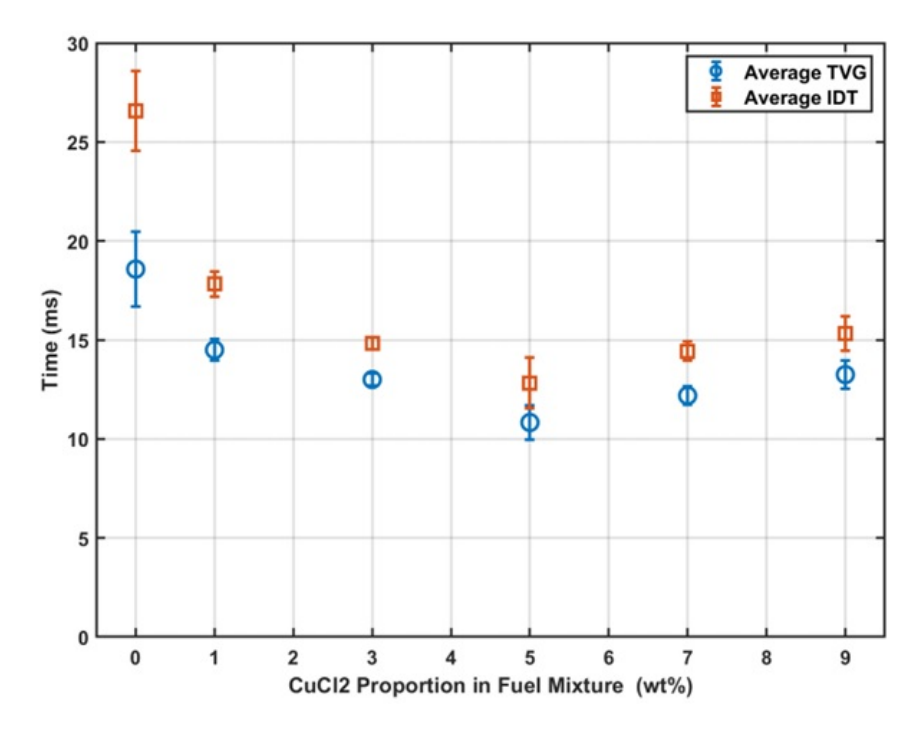


Figure 6: TVG and IDT measurements of various $CuCl_2$ additive proportions of DMTF in drop tests conducted with 95.41 ± 0.27 wt% HTP.

By 250 mm, TVG is reduced to around 12.5 ms, while IDT stabilises at approximately 13.8 ms. These results suggest that increasing the drop height enhances the kinetic energy of the HTP drop, and thus the mixing and decomposition processes, leading to shorter ignition times. This suggests that shorter TVG and IDT could be expected in injector tests, where mixing efficiency can be better than drop tests. It is worth noting that in the experiments conducted in [44] with a reactive fuel, drop height did not appear to affect TVG or IDT.

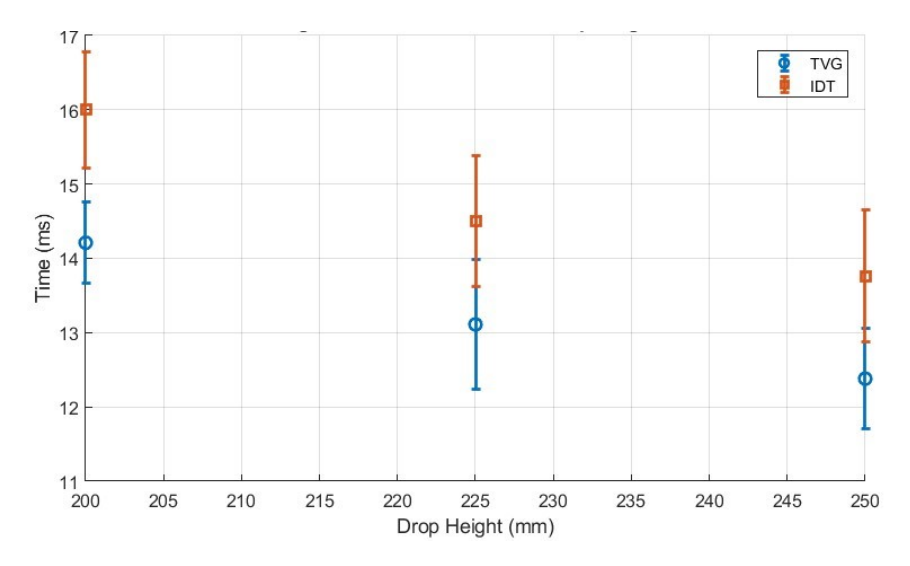


Figure 7: Effect of drop height on ignition characteristics of DMTF fuel mixtures with 95.41 ± 0.27 wt% HTP.

4.4 Effect of mixture ratio

In this subsection, the effect of mixture ratio (the ratio of the amount of oxidiser used in a drop test to the amount of fuel) on TVG and IDT is investigated. According to drop size measurements performed using PFV4 software, the average released HTP volume was 9.49 ± 0.67 microliters (μL). Fuel volume was measured with a micropipette, and mass calculated from the density of the fuel mixture.

Figure 8 presents average TVG and IDT across different mixture ratios, illustrating the effect of the propellant mixture ratio on the ignition characteristics of DMTF fuel mixtures in drop tests with 95.41 ± 0.27 wt% HTP. No significant variability was observed in TVG and IDT across mixture ratios between 0.99 and 4.55. Future studies could examine mixture ratios outside this range, and at lower HTP concentrations.

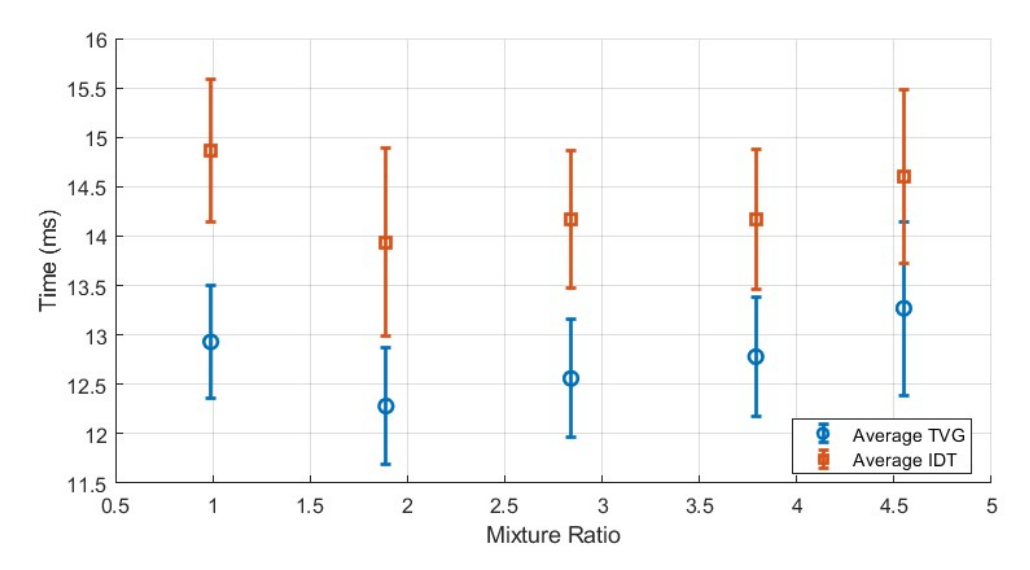


Figure 8: Effect of propellants mixture ratio on ignition characteristics of DMTF fuel mixtures for drop tests conducted with 95.41 ± 0.27 wt% HTP.

Other researchers tested a fuel mixture of [EMIM][SCN] and HTP, and found the IDT and TVG results remained similar across mass ratios [44]. However, in experiments using an amine-type fuel containing NaBH₄ with HTP, an increase in TVG was observed as the mixture ratio increased, but only when the HTP concentration was below 90 wt% [11,45].

4.5 Effect of test order (oxidiser onto fuel or fuel onto oxidiser)

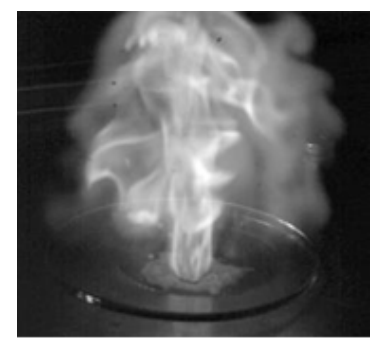
The positions of the oxidiser and fuel mixture were varied during the drop tests, with two configurations tested: HTP on the watch glass with fuel released from the syringe and fuel on the watch glass with HTP released from the syringe. The mixture ratio was 1.89 in all the tests but the total fuel and oxidizer amounts were slightly different due to equipment constraints. In the tests where fuel was dropped onto oxidiser, a significantly louder popping sound was observed, indicating a more vigorous initial reaction.

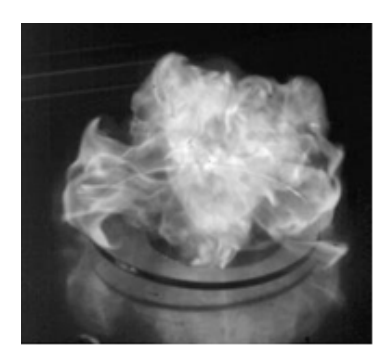
Table 6: Comparison of DMTF fuel mixtures with 95.41 ± 0.27 wt% HTP under different test orders.

Parameter/Test Condition	Ox on Fuel	Fuel on Ox
Fuel Mixture Volume (μl)	6.00	9.49
Oxidiser Volume (μ l)	9.49	15.00
Mixture Ratio	1.89	1.89
Test Order	Ox on Fuel	Fuel on Ox
Average TVG (ms)	13.33	21.86
TVG Standard Deviation (ms)	0.97	1.51
Average IDT (ms)	14.93	24.52
IDT Standard Deviation (ms)	1.18	1.69

The data from these drop tests are presented in Table 6. TVG was approximately 8 ms longer, and IDT approximately 10 ms longer, when the fuel mixture was released from the syringe, compared to the opposite configuration. This suggests that the primary difference between the two cases lies in the TVG process, which is largely influenced

by physical delay, which in turn is affected by the viscosity, surface tension and miscibility of the propellants [46], all of which influence the interaction dynamics between the fuel and oxidiser.





(a) Fuel released onto oxidiser

(b) Oxidiser released onto fuel

Figure 9: Effect of propellant release order on IDT.

In this study, viscosity measurements have not yet been performed. However, the literature shows that the addition of metal salt additives to liquid fuels tends to increase the viscosity of the fuel mixture. For example, the addition of 5 wt% CuSCN to [EMIM][SCN] increases the viscosity from 20.1 mPa s to 29.6 mPa s at 25 °C [4]. Similarly, the addition of copper(II) nitrate (CN) to monoethanolamine (MEA) based fuel significantly increases the kinematic viscosity, from 30.07 cSt at 1% CN to 119.14 cSt at 20% CN [40]. Thus, the fundamental difference in TVG values is thought to be due to the higher viscosity of the fuel mixture compared to the oxidiser, as it contains CuCl₂.

When the fuel came into contact with the oxidiser pool on the watch glass, the mixing, atomisation and reaction occur more slowly, prolonging the time required for sufficient heat generation to initiate vaporisation. Similar trends in IDT have been reported in the literature [12, 44, 47, 48]. Additionally, the fuel mixture remained concentrated in the area where the drop initially landed, rather than spreading quickly, as illustrated in Figure 9.

4.6 Test medium comparison (watch glass or test tube)

Further tests were conducted to investigate whether using a watch glass or a test tube had any effect on the TVG and IDT values (with DMTF with 6 wt% CuCl₂ as the fuel mixture, with a mixture ratio of 1.9 and a drop height of 250 mm). Data for this test are given in Table 7, and indicate that both TVG and IDT values are consistently higher in the glass tube compared to the watch glass. On average, TVG in the glass tube is approximately 3.5 ms longer, while IDT is 4 ms longer. The drop test results are shown in Figure 10.

Table 7: Comparison of DMTF fuel mixtures with 95.41 ± 0.27 wt% HTP in watch glass and test tube.

Parameter/Test Medium	Watch Glass	Glass Tube
Average TVG (ms)	12.52	16.00
TVG Standard Deviation (ms)	0.73	0.73
Average IDT (ms)	13.95	18.08
IDT Standard Deviation (ms)	0.60	0.68

One possible explanation is that when using the watch glass, local mixing could have been enhanced, and in turn enhance ignition. For the test tube, it may be that more thorough mixing occurs before ignition, which could explain the greater pop noticed during the tests. Another possible explanation is that atmospheric oxygen may contribute to the ignition, as suggested in [49]. In this case, more oxygen reaching the reaction site in the watch glass setup, with its wider surface area, could partly account for the faster reaction observed in that case.

4.7 Fourier transform infrared spectroscopy (FTIR)

In Fourier transform infrared spectroscopy (FTIR) spectroscopy, infrared (IR) radiation is passed through a sample, and the amount of each wavelength absorbed is measured. The resulting spectrum represents molecular 'fingerprint' of the sample. FTIR analysis can be applied to solids, liquids or gases [50].

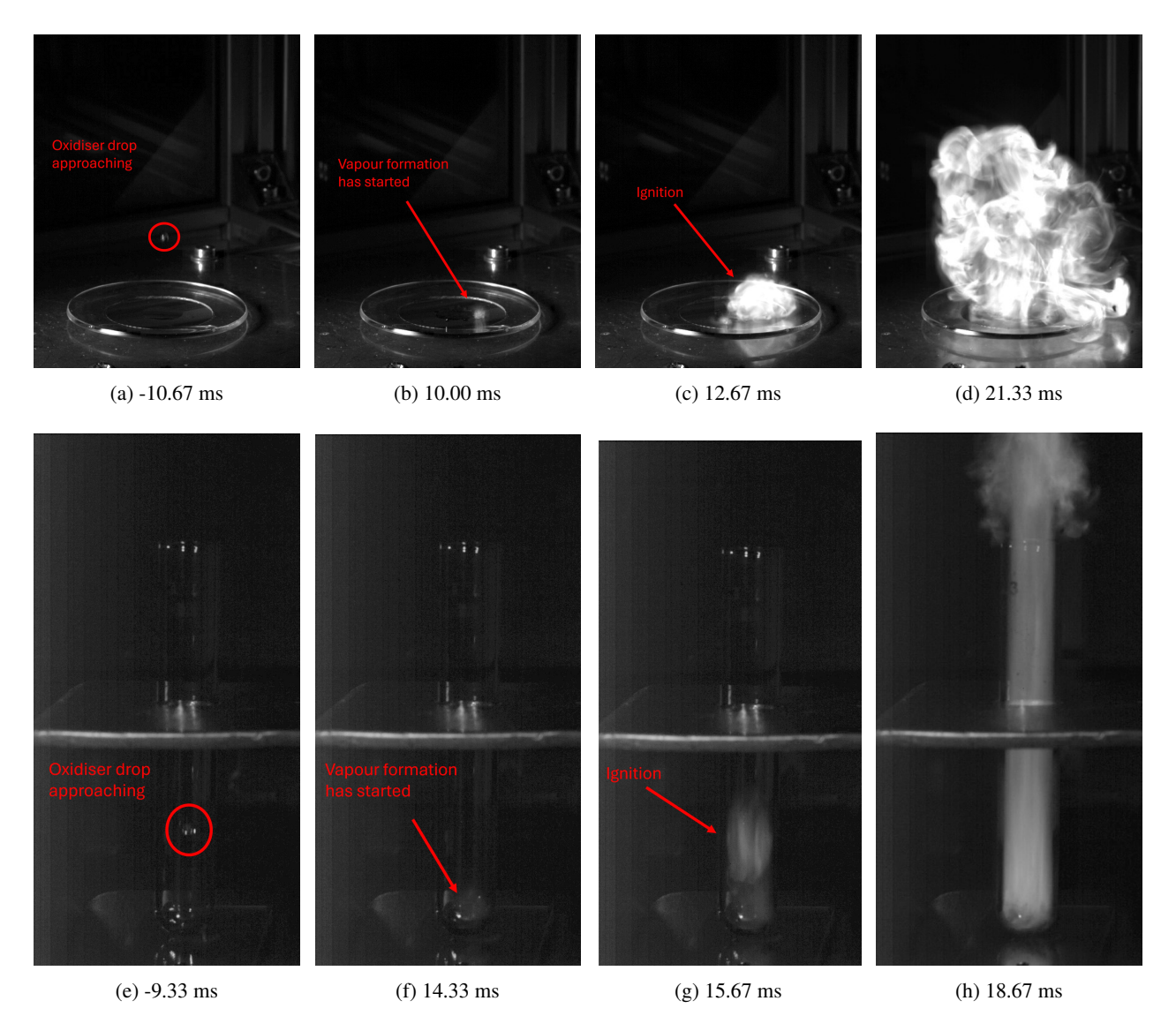


Figure 10: Snapshots of drop tests. Top row: conducted on a watch glass. Bottom row: conducted in a test tube. Each sequence shows the oxidiser drop approach, vapour formation, ignition, and combustion.

FTIR and similar techniques have been widely used to study the structural stability of fuel mixtures over time [12,51]. One study used FTIR to analyse the chemical stability of a fuel mixture containing N-methylimidazole, N-methyldiethanolamine and a $CuCl_2$ - $2H_2O$ catalyst, with no signs of chemical degradation between fresh and one-month-old samples [52]. Similarly, FTIR spectroscopy has been applied to examine the stability of a catalytic additive prepared for the [EMIM][BH₃CN] ionic liquid with HTP, and found that when fresh and 30-day-old fuel samples were compared, the only chemical change detected was a variation in the permeability of the $C \equiv N$ bond [12]. In another study, FTIR analysis was performed for a fuel mixture of [EMIM][SCN] and 5 wt% CuSCN, showing that the fuel mixture formed an ionic liquid containing the EMIM+ cation, SCN- and complex copper thiocyanate anions [4]. FTIR analysis can thus be carried out at specific intervals to investigate whether a fuel mixture undergoes any chemical changes over time, such as the formation of new bonds. These findings highlight the potential for chemical interactions in fuel mixtures containing catalytic additives, and demonstrate the effectiveness of FTIR in assessing chemical stability, providing valuable insight into fuel composition over time.

FTIR spectroscopy was conducted for $CuCl_2$, DMTF and a 5 wt% solution of $CuCl_2$ in DMTF, using a Thermo Scientific Nicolet iS5 spectrometer equipped with an iD7 ATR attachment. All measurements were conducted at the School of Chemistry and Chemical Engineering at the University of Southampton. Figure 11 presents these three FTIR spectra. The top spectrum corresponds to $CuCl_2$, displaying characteristic absorption peaks. The middle spectrum is that of pure DMTF, showing the absorption bands. The bottom spectrum is of the 5wt% solution of $CuCl_2$ in DMTF. The peaks observed at 518, 822, 913, 965, 1050, 1205, 1394, 1412, 1440, 1463, 1532, 2357, 2797, 2899 and 2938 cm⁻¹

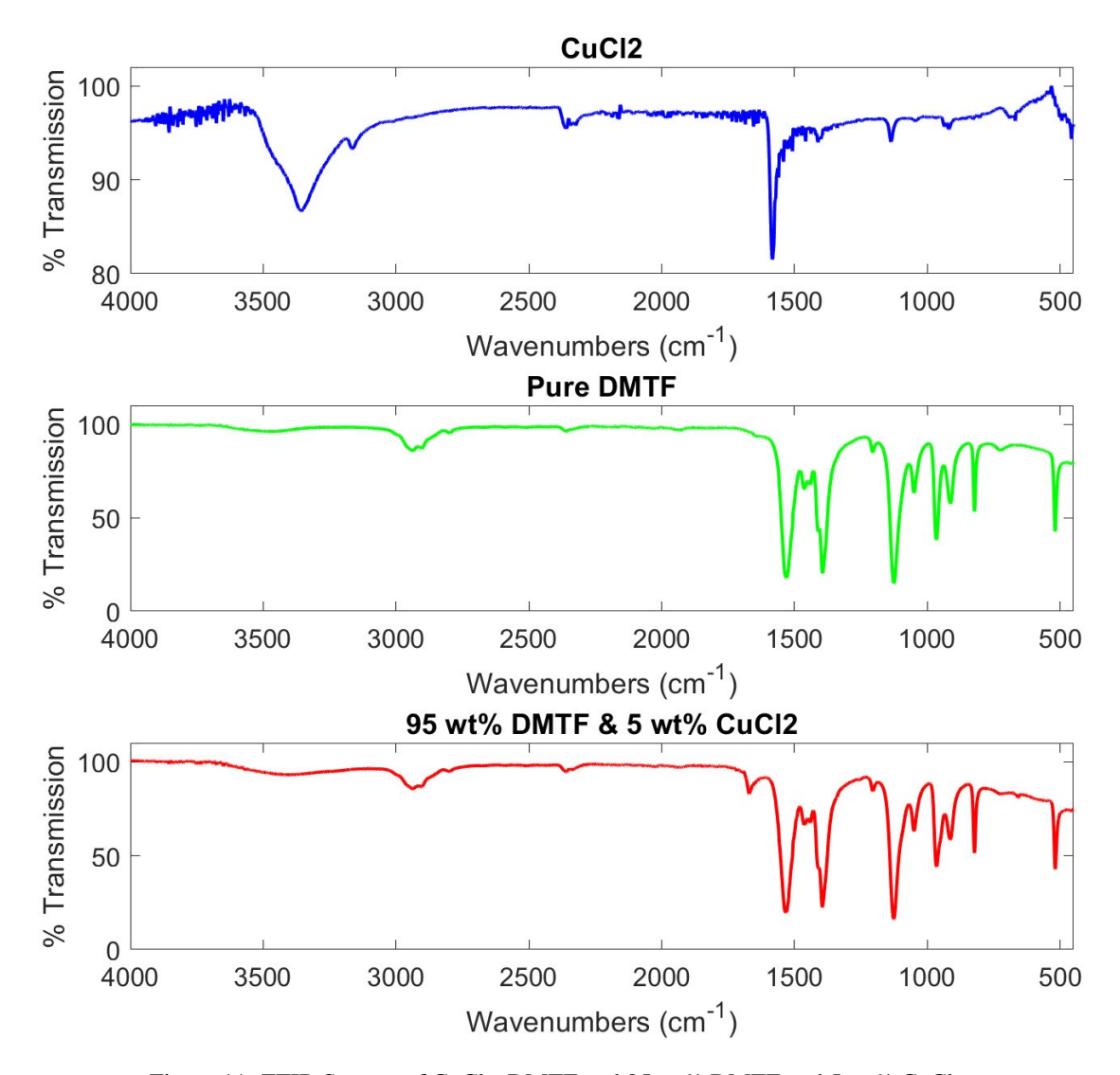


Figure 11: FTIR Spectra of CuCl₂, DMTF and 95 wt% DMTF and 5 wt% CuCl₂.

were consistent between pure DMTF and the solution of CuCl₂ in DMTF. However, a new peak was detected at 1670 cm⁻¹, which is commonly associated with C=O stretching in dimethylformamide [53,54], suggesting the formation of a new chemical complex in the solution.

To confirm the long-term stability of the CuCl₂-DMTF fuel mixture, a detailed chemical stability analysis is required. Additionally, spectroscopy can provide deeper insight into its composition and potential reactions. Further research can explore new fuel formulations by testing DMTF with alternative additives, such as CuSCN.

5. Conclusion and Future Work

This study assessed the potential of DMTF and HTP as a green bipropellant combination for spacecraft propulsion. NASA CEA simulations showed that the DMTF/HTP system yields a maximum vacuum specific impulse of approximately 316 s and a peak density-specific impulse of $422\,\mathrm{g\cdot s/cm^3}$, exceeding the volumetric efficiency of conventional MMH/NTO despite slightly lower energetic performance. Drop tests confirmed reliable hypergolic ignition, with the addition of 6 wt% CuCl₂ reducing TVG and IDT to $12.13\pm0.83\,\mathrm{ms}$ and $13.71\pm0.86\,\mathrm{ms}$, respectively. Test conditions such as drop height, release sequence and test medium were also shown to influence ignition behaviour.

The next step of the project is to perform injector tests to determine the ignition and combustion of the determined propellant combinations in flow conditions. Toward this end, a simple material compatibility study will be performed for DMTF, and solutions of CuCl₂ in DMTF. The injector test mechanism is being developed according to the materials identified in the compatibility tests. Thruster tests will be performed according to the results obtained from the injector tests.

6. Acknowledgments

The corresponding author gratefully acknowledges the financial support provided by a scholarship from the Republic of Türkiye Ministry of National Education. The authors also wish to thank Dr Rachel McKerracher and Dr Boomadevi Shanmugam for granting access to laboratory facilities at the University of Southampton; Dr Andrew Robinson, Mr Stuart Findlow and Mrs Aga Murch from the Testing and Structures Research Laboratory (TSLR) for their support in providing essential high-speed photography equipment and instruction in its use; and Dr Robert Bannister for his assistance with the FTIR spectrometer at the School of Chemistry and Chemical Engineering.

References

- [1] G.P. Sutton and O. Biblarz. Rocket Propulsion Elements. A Wiley Interscience publication. Wiley, 2017.
- [2] Merck Life Science UK Limited. Safety data sheet: Methylhydrazine (product number: M50001). *Safety Data Sheet, Aldrich, Merck Life Science UK Limited*, March 2024. Version 8.13, Revision Date: 08 March 2024.
- [3] GHC Gerling, Holz & Co. Handels GmbH. Safety data sheet: Dinitrogen tetraoxide. *Safety Data Sheet, GHC Gerling, Holz & Co. Handels GmbH*, May 2023. Version 12.0, Revision Date: 30 May 2023.
- [4] Felix Lauck, Jakob Balkenhohl, Michele Negri, Dominic Freudenmann, and Stefan Schlechtriem. Green bipropellant development a study on the hypergolicity of imidazole thiocyanate ionic liquids with hydrogen peroxide in an automated drop test setup. *Combustion and Flame*, 226:87–97, 2021.
- [5] European Chemicals Agency (ECHA). Hydrazine substance information, 2024. Accessed: 2025-05-24.
- [6] R. K. Palmer and J. J. Rusek. Low-Toxicity Reactive Hypergolic Fuels for Use with Hydrogen Peroxide. In A. Wilson, editor, *ESA Special Publication*, volume 557 of *ESA Special Publication*, page 32.1, October 2004.
- [7] Sh. L. Guseinov, S. G. Fedorov, V. A. Kosykh, and P. A. Storozhenko. Hypergolic propellants based on hydrogen peroxide and organic compounds: historical aspect and current state. *Russian Chemical Bulletin*, 67(11):1943–1954, November 2018.
- [8] Timothee Pourpoint. Hypergolic ignition of a catalytically promoted fuel with rocket grade hydrogen peroxide. *ETD Collection for Purdue University*, 01 2005.
- [9] Rohit Mahakali, Fred Kuipers, Allen Yan, William Anderson, and Timothee Pourpoint. Development of reduced toxicity hypergolic propellants. In 47th AIAA/ASME/SAE/ASEE Joint Propulsion Conference & Exhibit, July 2011.
- [10] Brandon K. Kan, Stephen D. Heister, and Daniel E. Paxson. Experimental study of pressure gain combustion with hypergolic rocket propellants. *Journal of Propulsion and Power*, 33(1):112–120, 2017.
- [11] Keigo Hatai and Taiichi Nagata. Quantitative clarification of stable ignition region for hkp110 green hypergolic bipropellant. *Aerospace*, 9(3), 2022.
- [12] Vikas K. Bhosale, Junyeong Jeong, Jonghoon Choi, David G. Churchill, Yunho Lee, and Sejin Kwon. Additive-promoted hypergolic ignition of ionic liquid with hydrogen peroxide. *Combustion and Flame*, 214:426–436, 4 2020.
- [13] Vikas K. Bhosale, Kyu-Seop Kim, Sejin Kwon, and David G. Churchill. Sodium iodide: a trigger for hypergolic ignition of non-toxic fuels with hydrogen peroxide. *AIAA Propulsion and Energy 2020 Forum*, 2020.
- [14] Vikas K. Bhosale, Keonwoong Lee, Hosung Yoon, and Sejin Kwon. Green bipropellant: Performance evaluation of hypergolic ionic liquid-biofuel with hydrogen peroxide. *Fuel*, 376:132688, 2024.
- [15] Hyeonjun Im, Vincent Mario Pierre Ugolini, Junyeong Jeong, and Sejin Kwon. Spray combustion visualization of spray-impinging injector for low-toxic hypergolic fuel and h₂o₂. In *Proceedings of Space Propulsion Conference* 2024. KAIST, 2024. SP2024_204.
- [16] Kyu-Seop Kim, Sangwoo Jung, and Sejin Kwon. Optical visualization of hypergolic burning spray structure using blue light spectrum. *Acta Astronautica*, 193:230–236, 2022.

- [17] Hongjae Kang, Dongwook Jang, and Sejin Kwon. Demonstration of 500 n scale bipropellant thruster using non-toxic hypergolic fuel and hydrogen peroxide. *Aerospace Science and Technology*, 49:209–214, 2016.
- [18] Hongjae Kang and Sejin Kwon. Development of 500 n scale green hypergolic bipropellant thruster using hydrogen peroxide as an oxidizer. In 51st AIAA/SAE/ASEE Joint Propulsion Conference, 2015.
- [19] Hongjae Kang and Sejin Kwon. Green hypergolic combination: Diethylenetriamine-based fuel and hydrogen peroxide. *Acta Astronautica*, 137:25–30, 2017.
- [20] Michele Negri and Felix Lauck. Hot firing tests of a novel green hypergolic propellant in a thruster. *Journal of Propulsion and Power*, 38:1–11, 01 2022.
- [21] S. Morales Jimenez, R. Beaver, and T. L. Pourpoint. The influence of chemical descriptors on the reactivity of potential hypergolic fuels with hydrogen peroxide. JANNAF 70th JPM/PIB/48th SMBS/44th PEDCS/33rd SEPS/17th MSS/1st HTMAS Joint Subcommittee Meeting, 2023.
- [22] L. M. Kamperschroer. *Development and Characterization of Thio-Amide-Based Hypergolic Fuels*. PhD thesis, Purdue University Graduate School, 2020.
- [23] Grzegorz Rarata and Wojciech Florczuk. Safety aspects of hypergolic propellants with hydrogen peroxide. *Materialy Wysokoenergetyczne / High Energy Materials*, 9:136–144, 12 2017.
- [24] ChemEurope. High-test peroxide, 2025. Accessed: 20-Feb-2025.
- [25] CF Industries. Dinitrogen tetroxide, mixed oxides of nitrogen safety data sheet, 2024. Revision Date: 4 June 2024.
- [26] Evonik Resource Efficiency GmbH. Safety data sheet for propulse 980 htp. Material Safety Data Sheet (MSDS), 2016. Version 2.8, Revision Date: 05.08.2016.
- [27] Stefania Carlotti and Filippo Maggi. Evaluating new liquid storable bipropellants: Safety and performance assessments. *Aerospace*, 9(10), 2022.
- [28] NASA. Fire, explosion, compatibility and safety hazards of hydrogen peroxide. Technical manual, National Aeronautics and Space Administration (NASA), 2004. Accessed: February 23, 2025.
- [29] Evonik Active Oxygens. Physico-chemical properties of hydrogen peroxide, 2025. Accessed: 18-Feb-2025.
- [30] NOAA Chemical Database. Nitrogen oxides (nox) chemical reactivity and hazards information, n.d. Accessed: March 2, 2025.
- [31] National Center for Biotechnology Information. Nitrogen tetroxide pubchem, 2025. Accessed: March 2, 2025.
- [32] National Institute of Standards and Technology (NIST). Methylhydrazine: Thermochemical data. https://webbook.nist.gov/cgi/cbook.cgi?Source=1951AST%2FFIN1939&Mask=7, 2025. Accessed: 2025-05-16.
- [33] Merck Life Science UK Limited. Safety Data Sheet: N,N-Dimethylthioformamide. https://www.sigmaaldrich.com/GB/en/sds/aldrich/163643, 2025. Product Number: 163643, Version 6.4, Revision Date: 25 April 2025.
- [34] P.O. Dunstan and L.C.R. dos Santos. Thermochemistry of amide and thioamide complexes of arsenic trihalides. *Thermochimica Acta*, 156:163–177, 1989.
- [35] N,n-dimethylthioformamide (cas 758-16-7) chemical information. https://www.chemsrc.com/en/cas/758-16-7_1137910.html, 2025. Accessed: 16 May 2025.
- [36] PubChem. N,n-dimethylthioformamide. https://pubchem.ncbi.nlm.nih.gov/compound/N_N-Dimethylthioformamide#section=3D-Conformer, 2024. Accessed: 2025-05-26.
- [37] S. Gordon. Computer Program for Calculation of Complex Chemical Equilibrium Compositions and Applications. Part 1: Analysis. NASA Reference Publication (RP), 1994.
- [38] Bonnie J. McBride and Sanford Gordon. Computer program for calculation of complex chemical equilibrium compositions and applications ii. users manual and program description. NASA Reference Publication (RP) NASA-RP-1311, NASA Lewis Research Center, Cleveland, OH, United States, June 1996. Public Use Permitted.

- [39] ARIANE Group. Chemical bi-propellant thruster family: 10n, 200n, 400n. Technical report, Ariane Group, n.d. Accessed: 2025-02-21.
- [40] Stefania Carlotti, Luca Caffiero, Davide Orlandi, and Filippo Maggi. Hypergolic ignition of amine-based fuels with hydrogen peroxide. In *Aerospace Europe Conference 2023 10th EUCASS 9th CEAS*, 2023.
- [41] Joshua M. Hollingshead, Makayla L.L. Ianuzzi, Jeffrey D. Moore, Richard A. Yetter, and Grant A. Risha. Investigation of ignition delay and combustion efficiency of tmeda and various concentrations of nitric acid. *AIAA Propulsion and Energy 2020 Forum*, pages 1–9, 2020.
- [42] Fabio A.S. Mota, Lihan Fei, Chenglong Tang, Zuohua Huang, and Fernando S. Costa. Hypergolic ignition behaviors of green propellants with hydrogen peroxide: The tmeda/dmea system. *Fuel*, 336:127086, 2023.
- [43] B. Austin, W. Anderson, and S. Heister. Characterization of pintle engine performance for nontoxic hypergolic bipropellants. *Journal of Propulsion and Power J PROPUL POWER*, 21:627–635, 07 2005.
- [44] Felix Lauck, Jakob Balkenhohl, Michele Negri, Dominic Freudenmann, and S. Schlechtriem. Ignition investigations of a novel hypergolic ionic liquid with hydrogen peroxide in drop tests. In 7TH SPACE PROPULSION CONFERENCE 2020+1, 03 2021.
- [45] Keigo Hatai. Recent progress on green hypergolic bipropellant research in jaxa. In *Space Propulsion Conference 2024*, Tsukuba Space Center, 2-1-1 Sengen, Tsukuba, Ibaraki, JAPAN, 2024. Japan Aerospace Exploration Agency (JAXA). Accessed: 16-Feb-2025.
- [46] T.L. Pourpoint and W.E. Anderson. Hypergolic ignition of catalytically promoted fuels with rocket hydrogen peroxide. In *European Conference for Aerospace Sciences (EUCASS)*, West Lafayette, United States, 2004. Purdue University School of Aeronautics and Astronautics.
- [47] Hongjae Kang, Eunkwang Lee, and Sejin Kwon. Suppression of hard start for nontoxic hypergolic thruster using h2o2 oxidizer. *Journal of Propulsion and Power*, 33:1–7, 02 2017.
- [48] Jakob Balkenhohl. Design, construction and commissioning of a reaction chamber for hypergolic fuels as well as first optical measurements of the flame emission. Master's thesis, University of Stuttgart, Institute of Space Systems, Stuttgart, Germany, 2019. IRS-19-S-056.
- [49] Souvick Biswas, Kazuumi Fujioka, Ivan Antonov, Grace L. Rizzo, Steven D. Chambreau, Stefan Schneider, Rui Sun, and Ralf I. Kaiser. Hypergolic ionic liquids: To be or not to be? *Chem. Sci.*, 15(4):1480–1487, 2024.
- [50] Dmitry Fishman. *FTIR Principles*. Thermo Nicolet Corporation, 2001. 2001 Thermo Nicolet Corporation. All rights reserved, worldwide. Accessed: 13 Feb. 2025.
- [51] Seonghyeon Park, Kyounghwan Lee, Hongjae Kang, Youngchul Park, and Jongkwang Lee. Effects of oxidizing additives on the physical properties and ignition performance of hydrogen peroxide-based hypergolic propellants. *Acta Astronautica*, 200:48–55, 2022.
- [52] Fabio A.S. Mota, Mingyang Liu, Abrar A.A. Mohsen, Xiaoxin Yao, Zhaoming Mai, and Chenglong Tang. Development of polyamine/alkanolamine-based hypergolics with hydrogen peroxide: A new route to n-methylimidazole with mdea as a promising green fuel. *Fuel*, 357:129798, 2024.
- [53] Ying-Ke Ren, Shi-Dong Liu, Bin Duan, Ya-Feng Xu, Zhao-Qian Li, Yang Huang, Lin-Hua Hu, Jun Zhu, and Song-Yuan Dai. Controllable intermediates by molecular self-assembly for optimizing the fabrication of large-grain perovskite films via one-step spin-coating. *Journal of Alloys and Compounds*, 705:205–210, 2017.
- [54] Nathalia Hammes, Claver Pinheiro, Iran Rocha Segundo, Natalia Candido Homem, M. M. Silva, Helena P. Felgueiras, Graca M. B. Soares, Elisabete Freitas, Manuel F. M. Costa, and Joaquim Alexandre O. Carneiro. Coaxial fibres incorporated with phase change materials for thermoregulation applications. *Applied Sciences*, 14(6), 2024.